



Selective oxidation of olefins with aqueous hydrogen peroxide over phosphomolybdic acid functionalized knitting aryl network polymer



Xiaojing Song^a, Wanchun Zhu^a, Yan Yan^b, Hongcheng Gao^a, Wenxiu Gao^a,
Wenxiang Zhang^a, Mingjun Jia^{a,*}

^a Key Laboratory of Surface and Interface Chemistry of Jilin Province, College of Chemistry, Jilin University, 130021 Changchun, China

^b State Key Laboratory of Inorganic Synthesis and Preparative Chemistry, College of Chemistry, Jilin University, Changchun 130012, China

ARTICLE INFO

Article history:

Received 8 September 2015

Received in revised form 5 December 2015

Accepted 17 December 2015

Available online 23 December 2015

Keywords:

Phosphomolybdic acid

Knitting aryl network polymer

Immobilization

Selective oxidation

Olefins

ABSTRACT

A phosphomolybdic acid (PMA)-based heterogeneous catalyst, denoted as PMA/KAP, was prepared by immobilizing PMA onto a knitting aryl network polymer (KAP) based on triphenylphosphine (PPh_3). The catalytic property of PMA/KAP was investigated for the selective oxidation of olefins with aqueous hydrogen peroxide (H_2O_2) as oxidant. When using ethyl acetate (EAC) as reaction medium, PMA/KAP performs higher activity and selectivity to epoxide for a variety of olefins, and it can be reused for several times without obvious loss of activity. When the reaction was carried out in acetonitrile (AN) medium, deactivation of PMA/KAP catalyst can be observed immediately. A variety of characterization results suggest that the degradation of PMA unit to $(\text{PO}_4[\text{MoO}(\text{O}_2)_2]_4)^{3-}$ occurs easily when the PMA/KAP catalyst is operated in $\text{H}_2\text{O}_2/\text{AN}$ system, while such degradation behavior could be significantly inhibited when the catalyst is used in the system of $\text{H}_2\text{O}_2/\text{EAC}$. We proposed that the neighbouring P-containing ligands dispersed in the framework of KAP can produce a steric pocket with low electron density, which can promote the formation of multi-weak coordination interaction between PMA unit and several P ligands. Such multi-weak interaction can inhibit the degradation of PMA to $(\text{PO}_4[\text{MoO}(\text{O}_2)_2]_4)^{3-}$, thus avoiding the leaching of active species from the KAP support, and resulting in the formation of relatively stable heterogeneous PMA supported catalyst for olefin epoxidation with H_2O_2 in the media of EAC.

© 2015 Elsevier B.V. All rights reserved.

1. Introduction

Porous organic frameworks (POFs) have received increasing attention due to their unique properties like large surface, low skeletal density, and high chemical stability [1–10]. Compared with traditional inorganic materials, one particular advantage of POFs is its ability to introduce various organic chemical functionalities for constructing novel advanced materials. Recently, a variety of POFs containing functional units have been reported, which have shown potential applications in adsorption, ion exchange, nanotechnology, and catalysis [11–16].

Knitting aryl network polymers (KAPs) are a new family of POFs, which can be prepared though a simple one-step Friedel–Crafts reaction using aromatic compounds as the monomer and formaldehyde dimethyl acetal as the external cross-linker [17–19]. In the field of catalysis, a few recent works showed that a functionalized KAP material, obtained by knitting triphenylphosphine (PPh_3) and

benzene with an external cross-linker, could be used as suitable support to fabricate efficient heterogeneous catalysts. For instance, Pd nanoparticles supported PPh_3 -functionalized KAP exhibited excellent activity and selectivity for the Suzuki–Miyaura crossing coupling reaction of aryl chlorides [18]. Rh supported PPh_3 -based KAP showed higher activity and stability than Rh supported silica catalyst for the hydroformylation of higher olefins [20]. It was believed that the special coordinating ability of PPh_3 ligands as well as the porous characteristics of KAP play critical role in stabilizing the nanoparticles of noble metal.

Recently, numerous contributions have been made to develop highly active and stable polyoxometalates (POM)-based heterogeneous catalysts for the application in liquid-phase oxidation (or epoxidation) of olefins. By selecting different supports and preparation strategies, a variety of relatively active and stable POM-supported heterogeneous catalysts have been obtained [21–23]. For instance, Kholdeeva et al. immobilized $[\text{PW}_{11}\text{CoO}_{39}]^{5-}$ and $[\text{PW}_{11}\text{TiO}_{40}]^{5-}$ into MIL-101 through electrostatic interaction, and found that the resulting materials were active heterogeneous catalysts for the oxidation of olefins with H_2O_2 or O_2 as oxidant [21]. Bordoloi et al. reported that molybdoanophosphoric acids sup-

* Corresponding author. Fax: +86 431 85168420.

E-mail address: jiamj@jlu.edu.cn (M. Jia).

ported amine-modified mesoporous silicas, were highly active and stable catalysts for selective oxidation of anthracene with *t*-BuOOH as oxidant [22]. Kasai et al. immobilized [*r*-1,2-H₂SiV₂W₁₀O₄₀] on *N*-octyldihydroimidazolium cation-modified SiO₂, to obtain an efficient catalyst for the oxidation of olefins and sulfides with H₂O₂ as oxidant [23]. Our recent work showed that phosphomolybdic acid supported COF-300 (a covalent organic framework material) exhibits high activity and stability for the epoxidation of cyclooctene and 1-octene with *t*-BuOOH as oxidant [24]. In spite of these considerable progresses, most of the POM supported catalysts commonly suffer from active species leaching from the supports, which is particularly serious when H₂O₂ is used as oxidant [25]. This can be mainly attributed to the strong complexing and solvolytic properties of H₂O₂ and solvents, which can usually transfer PMA cluster into dissolvable compound, or turn it to smaller species by oxidative degradation [26,27]. Besides, it is quite hard to get truly heterogeneous supported POM catalysts, since the relatively large size of POM clusters brings serious difficulty to build stable linkages between supports and POM. Therefore, it is still a very significant subject to develop novel efficient POM-based heterogeneous catalysts for the oxidation of olefins with H₂O₂, and to reveal the key factors favoring the improvement of the stability of the POM supported catalysts.

In this work, we tried to use PPh₃-based KAP as support to prepare phosphomolybdic acid (PMA) supported heterogeneous catalyst, and the catalytic performance of the resulting material (PMA/KAP) was studied for the oxidation of olefins with H₂O₂ as oxidant in different reaction media. Besides, a homogeneous catalyst named PMA-(PPh₃)₃ was also prepared by coordinating PMA with free PPh₃ ligands for the purpose of comparison. By combining a variety of characterization results, it can be revealed that multi-interactions are present between one PMA unit and several P-containing ligands dispersed in the framework of KAP support, which can result in the formation of relatively active and stable PMA supported KAP catalyst for the epoxidation of olefins with H₂O₂ in the presence of EAC.

2. Experimental section

2.1. Materials

Benzene (PhH), triphenylphosphine (PPh₃), FeCl₃ (anhydrous), methanol, 1,2-dichloroethane (DCE), dimethylformamide (DMF), acetonitrile (AN), ethylacetate (EAC) and 30 wt% H₂O₂ aqueous solution were purchased from China National Medicines Corporation Ltd., all of which were of analytical grade and were used as received. Cyclooctene, cyclohexene, styrene, 1-hexene, 1-octene, *a*-piene and formaldehyde dimethylacetal (FDA) were purchased from Aldrich.

2.2. The preparation of catalysts

KAP was synthesized according to literature procedure [18]. Typically, 1.56 g PhH, 5.25 g PPh₃ and 4.56 g FDA were dissolved in 20 ml DCE containing 9.75 g FeCl₃ (anhydrous). The resulting mixture was stirred at 45 °C for 5 h to form original network, and then heated at 80 °C for 67 h to complete the reaction. The as-synthesized KAP was washed with methanol in a Soxhlet to remove residual FeCl₃. Catalyst PMA/KAP was prepared by adding 0.30 g KAP support into a methanol solution containing 0.053 g PMA, the mixture was then stirred for 24 h at room temperature. The resulting solid was washed three times with methanol, and then washed with methanol in a Soxhlet's extractor at 80 °C for 24 h, then dry in vacuum at 60 °C for 8 h. The PMA loading determined by atomic adsorption spectroscopy (AAS) was 0.05 mmol/g. The processes for

preparation of KAP and PMA/KAP are shown in Scheme 1. Element analysis (%): KAP, C 83.8, H 6.2, Fe 5.2. PMA/KAP: C 76.9, H 5.6, Fe 2.4.

For comparison, PMA-(PPh₃)₃ complex was synthesized through adding some PMA into a methanol solution containing PPh₃ ligands (the ratio of PPh₃/PMA is about 3.5). The mixed solution presents yellow at first, and the solid complex with light green color can be obtained finally after filtering and washing by CH₃OH. The resultant complex is denoted as PMA-(PPh₃)₃, in which the mole ratio of PMA/PPh₃ is determined by elemental analysis. The process for preparation of PMA-(PPh₃)₃ is shown in Scheme 2.

2.3. Catalytic reaction

The catalytic properties of PMA/KAP and PMA-(PPh₃)₃ were tested by the oxidation of olefins. The reactions were initiated by adding oxidant H₂O₂ into a 10 ml flask containing catalyst, solvent and corresponding reactants under beforehand designed temperature. The course of the reactions were monitored and quantified by Shimadzu GC-8A gas chromatograph with HP-5 capillary column.

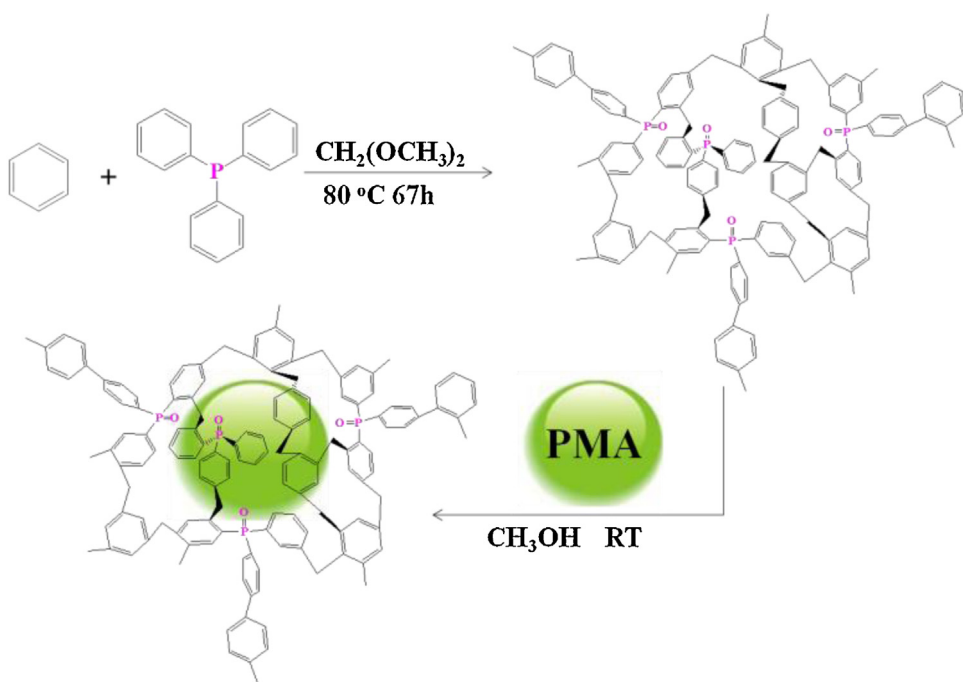
2.4. Characterization techniques

FT-IR spectra were recorded on a Nicolet AVATAR 370 DTGS spectrometer in the range 4000–500 cm⁻¹. Powder X-ray diffraction (XRD) patterns were recorded on a Shimadzu XRD-6000 diffractometer (40 kV, 30 mA), using Ni-filtered CuK α radiation. Thermogravimetry (TG) were carried out using A Netzsch Thermoanalyser STA 449F3 with a N₂ flow and heating rate of 10 °C/min, from room temperature to 800 °C. Transmission electron microscopy (TEM) images were taken with a H8100-IV electron microscope operating at 200 kV. The samples were suspended in ethanol by sonication and then picked up on a Cu grid covered with a carbon film. Element analyzes of C and H were implemented with a PerkinElmer 2400CHN elemental analyzer. For determining the Fe amount remained in KAP support or PMA/KAP catalyst, the sample was firstly treated by 3 M HNO₃ aqueous solution, and then the Fe concentration in the filtration was detected by inductively coupled plasma-optical emission spectroscopy (ICP-AES). N₂ adsorption/desorption isotherms were measured at 77 K using a Micromeritics ASAP 2010N analyzer. Samples were degassed at 110 °C for 8 h before measurements. Specific surface areas were calculated using BET model. XPS measurements were made on a VGESCA LAB MK-II X-ray electron spectrometer using Al K α radiation. Solid ³¹P MAS NMR spectra were recorded on a 400 MHZ Bruker spectrometer. The ³¹P MAS NMR chemical shifts are referenced to the resonances of monoammonium phosphate (NH₄H₂PO₄) standard. Liquid ³¹P NMR spectra were recorded on a 500 MHZ AVANCEIII500. ³¹P chemical shifts are referenced to 85% H₃PO₄ as an external standard.

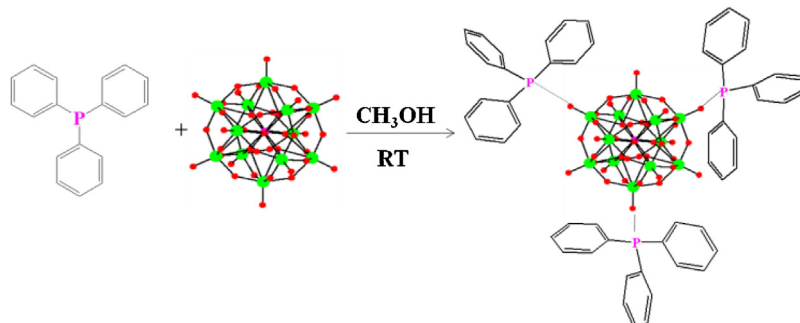
3. Results and discussion

3.1. Catalyst characterization

Fig. 1 shows the FT-IR spectra of KAP, PMA, PMA-(PPh₃)₃ and PMA/KAP. The characteristic bands of KAP are in agreement with the related literature results [18]. The benzene skeleton vibration peaks appear in the range of 1600–1450 cm⁻¹, while the peaks at around 1250–950 and 900–650 cm⁻¹ result from C–H bending vibrations of benzene ring. 1435 cm⁻¹ could be attributed to the P-CH₂ which shows that the phosphine ligands are embedded into the skeleton of KAP [28]. For PMA-(PPh₃)₃ and PMA/KAP, the characteristic bands of PMA appear in the range of 1100–700 cm⁻¹, confirming the presence of PMA units in the resulting catalysts.



Scheme 1. Preparation process of KAP support and PMA/KAP catalyst.



Scheme 2. Preparation process of PMA-(PPh_3)₃.

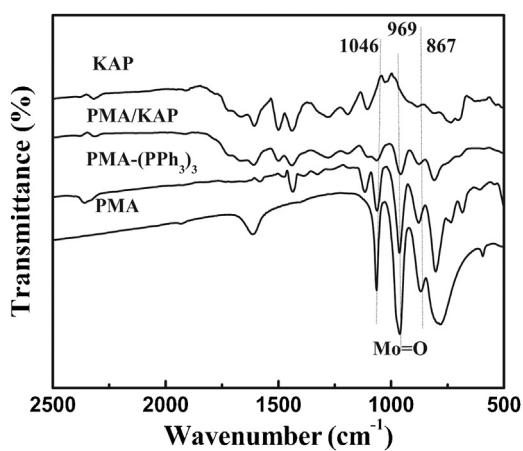


Fig. 1. FT-IR spectra of KAP, PMA, and PMA/KAP.

Fig. 2 reveals the XRD patterns of the PMA/KAP catalyst. There is only one broad peak, suggesting the amorphous characteristic of the resulting material. The absence of diffraction peaks associated with the crystalline phase of PMA suggests that PMA cluster should be highly dispersed on the surface or the channel of KAP support.

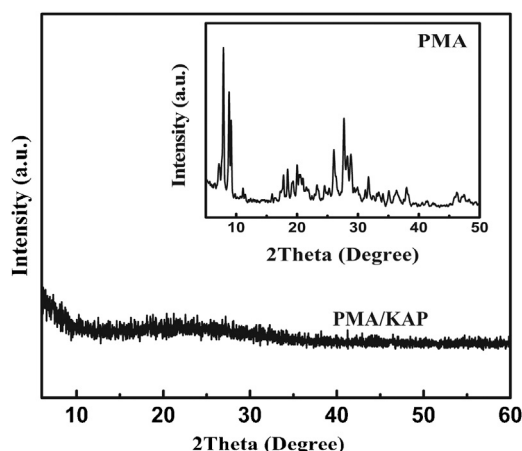


Fig. 2. The wide angle XRD patterns of PMA/KAP and pure PMA (insert).

TEM images of the KAP support and the PMA/KAP catalyst are shown in **Fig. 3**. Amorphous nanosize particles are observed in the image of the KAP support. Compared with the KAP support, the corresponding region of PMA/KAP turns to darker, which might be caused by the introduction of PMA units.

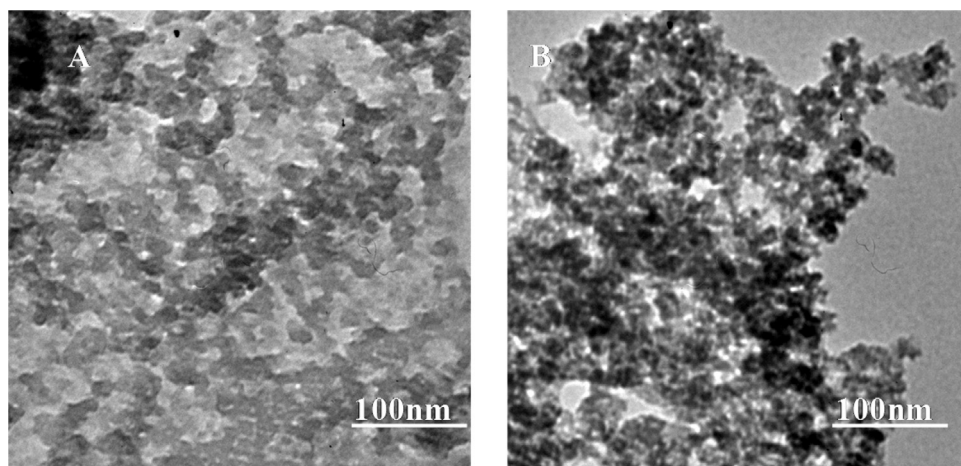


Fig. 3. The TEM images of (A) KAP and (B) PMA/KAP.

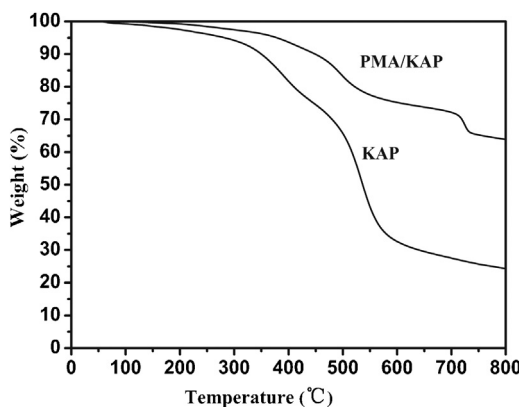


Fig. 4. TG analysis of PMA/KAP and KAP at a heating rate of 10 °C/min under nitrogen.

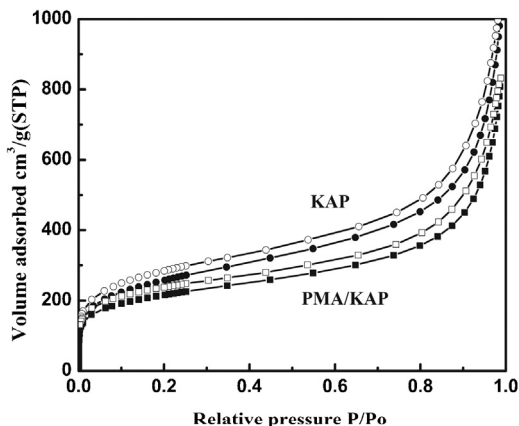


Fig. 5. Nitrogen adsorption and desorption isotherms of KAP and PMA/KAP.

The TG profiles of KAP and PMA/KAP are shown in Fig. 4. A slight weight loss at around 100 °C can be attributed to desorption of a trace amount of water and methanol. For KAP, significant weight loss starts at about 300 °C due to the thermal decomposition of this polymer support. The decomposition rate of PMA/KAP decreases somewhat in comparison with that of KAP support, which might be an indicative of the existence of some interactions between KAP support and PMA units.

The N₂ adsorption–desorption isotherms of KAP and PMA/KAP are shown in Fig. 5. For both samples, a steep nitrogen gas uptake at low relative pressure (0–0.1) can be observed, indicating the presence

of abundant micropores [18]. The appearance of hysteresis loop at relative pressure between 0.4 and 0.7 indicates the existence of a certain amount of mesopores in KAP and PMA/KAP. Moreover, a sharp rise at the high pressure regions (above 0.8) reveals the presence of macropores in these materials. Compared with KAP, the N₂ adsorption capacities for PMA/KAP decreases somewhat, which can be assigned to the introduction of PMA units to the surface/channel of KAP support. According to the traditional BET method, BET surface area of KAP is found to be 922 m²/g, and it decreases to 761 m²/g after introducing PMA.

The P 2p and Mo 3d XPS spectra of KAP, PMA, PMA-(PPh₃)₃ and PMA/KAP are shown in Fig. 6. The P 2p spectrum of KAP support shows a peak at 133.3 eV, which is higher than that of pure PPh₃ (132.2 eV), but quite consistent to the binding energy (BE) value for the reported triphenylphosphine oxide (OPPh₃) [29]. These results suggest that the P atoms in PPh₃ ligands have been oxidized to P=O species possibly by oxygen/FeCl₃ during the process for synthesizing KAP support. The spectrum of PMA shows a signal at 134.5, which is attributed to the BE of P in PMA. After supporting PMA on KAP, a broad peak centered at 133.8 can be observed, which should be due to the partial overlap of the P signals derived from KAP support and PMA. The Mo 3d XPS spectrum of PMA displays characteristic peaks at 236.3 and 233.2 eV, which are attributed to Mo (VI) 3d_{3/2} and Mo (VI) 3d_{5/2}, respectively [30]. For PMA-(PPh₃)₃, the binding energy of Mo shifts to more negatively (235.9 and 232.8 eV) than that of pure PMA, which can be attributed to the nucleophilic attack of the phosphine lone pair (in KAP) on a π* Mo=O orbital [31]. It is found that the Mo binding energies of PMA/KAP are similar to that of PMA-(PPh₃)₃, implying that the redox property of Mo species in both compounds are quite similar.

The ³¹P MAS-NMR spectra of PPh₃, PMA, KAP, PMA-(PPh₃)₃ and PMA/KAP are shown in Fig. 7. Free PPh₃ ligand and PMA display phosphorous resonance signals at -10.88 ppm and -4.84 ppm, respectively. For the P signal of PPh₃ ligand in PMA-(PPh₃)₃, it changes from -10.88 ppm (free PPh₃ ligand) to 1.33 ppm, suggesting that relatively strong coordination interaction should be built between the PPh₃ ligands and the PMA units. In previous literatures, it has been proposed that the phosphines (PR₃, R=Me, Et, Ph) might interact with the molybdenum (VI) oxides to form molybdenum complexes O=Mo=O ... PR₃ linkages [31–34]. The ³¹P NMR spectrum of KAP shows a broad signal centered at about 25 ppm, indicating that the chemical environment of P species in KAP is quite different from the pure PPh₃ ligand. These results suggest that the electron density of P species in KAP support decreases significantly after forming the knitting aryl network polymers, confirming further that the PPh₃ ligands have already been oxidized to

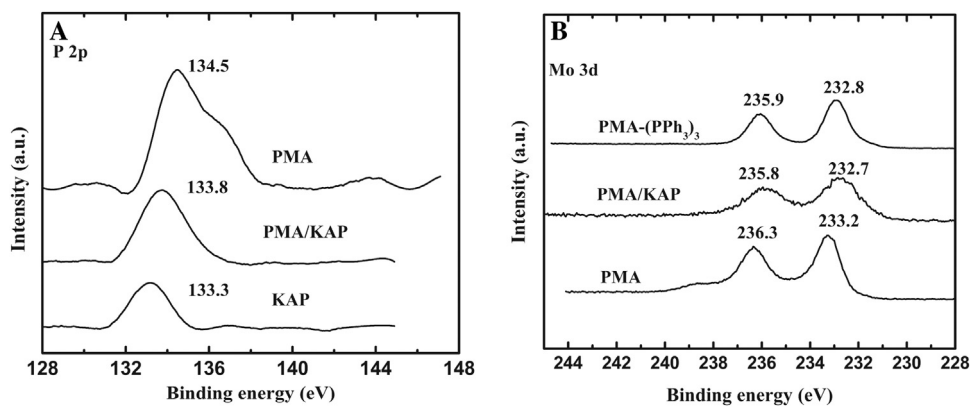


Fig. 6. XPS spectra for the BE of (A) P in KAP, PMA/KAP and PMA and (B) Mo in PMA, PMA/KAP and PMA-(PPh₃)₃.

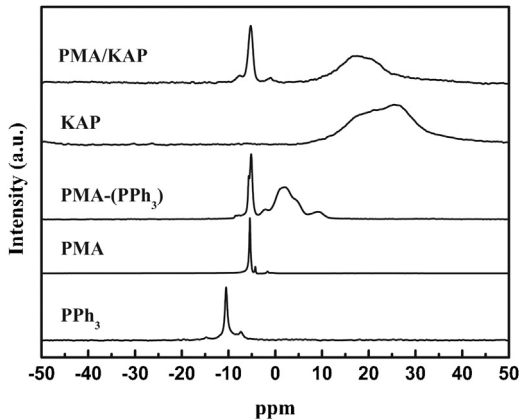


Fig. 7. ³¹P MAS-NMR spectrum of PPh₃, PMA, PMA-(PPh₃)₃, KAP and PMA/KAP.

OPPh₃ during the polymerizing process as revealed by the above XPS results. For both PMA/KAP and PMA-(PPh₃)₃, the P signals belonged to PMA are quite similar to the pure PMA, indicating that the basic structure of the introduced PMA units is remained. For the ³¹P NMR signal in KAP support, it shifts slightly toward high field after introducing the PMA units into the KAP support, suggesting the existence of weak coordination interaction between the Mo species in PMA units and the P atoms in KAP support. These results suggest that the OPPh₃ ligands existed in KAP support still have the coordination ability with the PMA units, thus may bring considerable effect on the structure stability (redox capacity) and the catalytic activity of the introduced PMA compounds.

3.2. Catalytic performance of PMA/KAP and PMA-(PPh₃)₃

The catalytic properties of PMA/KAP and PMA-(PPh₃)₃ were investigated for the oxidation of cyclooctene with H₂O₂ as oxidant in the presence of different solvent media (Table 1). Both PMA/KAP and PMA-(PPh₃)₃ are catalytically active for the epoxidation of cyclooctene. Compared with the homogeneous PMA-(PPh₃)₃, the solid PMA/KAP catalyst gives lower activity under test conditions. Moreover, the catalytic properties of both catalysts are solvent dependent, the conversion of cyclooctene follows the order of EAC > DMF > AN. When EAC is used as medium, PMA/KAP catalyst gives a 78.6% conversion of cyclooctene with nearly 100% selectivity of epoxide after 9 h reaction.

In addition, PMA/KAP and PMA-(PPh₃)₃ are also catalytically active for the oxidation/epoxidation of other olefins as shown in Table 2. They can even oxidize the relative inert terminal olefins of 1-hexene and 1-octene to their corresponding epoxides. For

Table 1

The oxidation results of cyclooctene with H₂O₂ as oxidant, PMA/KAP and PMA-(PPh₃)₃ as catalysts in different solvents.

Catalyst	Reaction media	Time (h)	Conversion (%)	Selectivity (%)	
				Epoxide	Diols
PMA/KAP	DMF	9	36.9	>99	–
PMA-(PPh ₃) ₃			56.0	>99	–
PMA/KAP	AN	9	26.4	>99	–
PMA-(PPh ₃) ₃			89.0	>99	–
PMA/KAP	EAC	9	78.6	>99	–
PMA-(PPh ₃) ₃		3	95.9	93.6	6.4

Reaction conditions: catalyst 10 mg, solvent 2 ml, cyclooctene 0.12 ml, H₂O₂ 0.30 ml, temperature 70 °C.

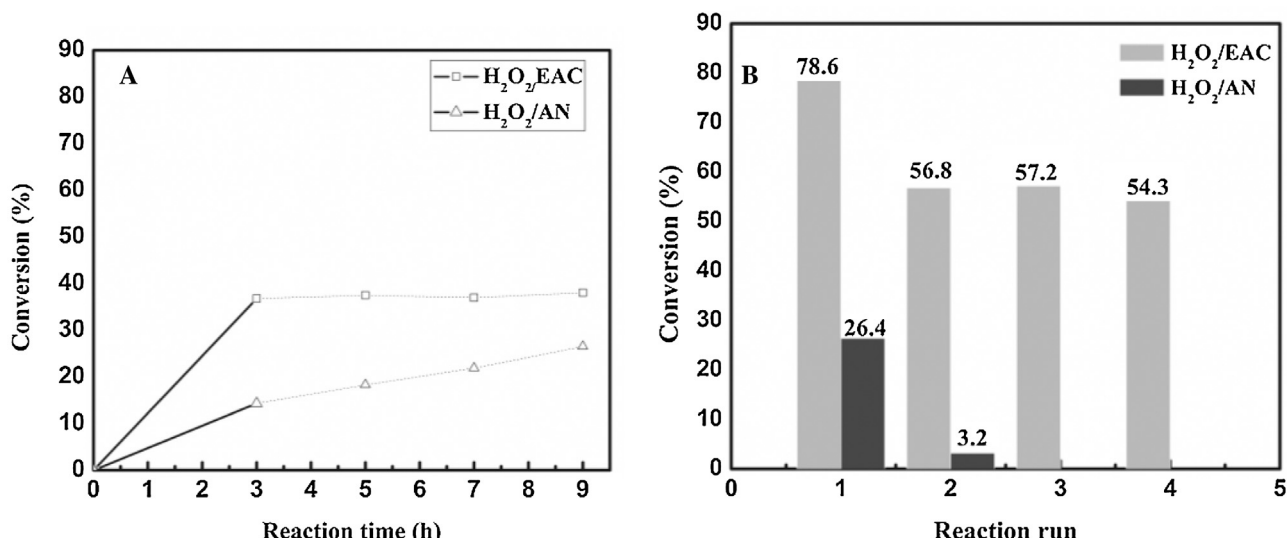
PMA/KAP, 1-hexene can be converted to epoxide rapidly, and 70.2% of conversion with >99% selectivity of epoxide is obtained. The conversion of 1-octene is rather low (10.6%) under the test conditions, possible due to the fact that the molecular of 1-octene has larger steric hindrance (caused by the increase of chain length). Notably, PMA/KAP exhibits much higher selectivity to 1-hexene epoxide than that of PMA-(PPh₃)₃, although the catalytic activity of PMA/KAP is slightly lower than the corresponding homogenous catalyst. Similar situation can also be observed for the epoxidation of styrene, in which PMA/KAP establishes lower activity but higher epoxide selectivity than that of PMA-(PPh₃)₃. Besides, PMA/KAP is also active for the oxidation of α -olefins and cyclohexene, which can convert the olefins to the corresponding epoxide and enol (or enone).

For studying the stability of PMA/KAP catalyst, leaching test was conducted in the system of H₂O₂/EAC or H₂O₂/AN. In duplicate reaction, the solid catalyst was separated by hot filtration, and the filtrate was then further stirred. As shown in Fig. 8A, no further conversion of cyclooctene could be detected in the filtrate for catalyst PMA/KAP in the system of H₂O₂/EAC, which demonstrates that the oxidation reaction is a truly heterogeneous process. As for the H₂O₂/AN system, cyclooctene can still be converted to epoxide rapidly after removing the PMA/KAP catalyst by filtrating, suggesting that leaching of active sites from the solid catalyst occurs during the reaction course. These results suggest that different solvent/oxidant systems can bring serious difference in influencing the stability of PMA/KAP catalyst.

The recycling experiments of PMA/KAP for cyclooctene epoxidation were carried out in the systems of H₂O₂/EAC and H₂O₂/AN. Before reusing, the recovered catalysts were washed with corresponding solvent and dried at 60 °C. In the system of H₂O₂/EAC, the activity of the recycled PMA/KAP catalyst decreases somewhat at the second run, it then keeps nearly consistent with further run. These results suggest that catalyst PMA/KAP is recyclable in the

Table 2The oxidation of olefins catalyzed by PMA/KAP and PMA-(PPh₃)₃ with H₂O₂ as oxidant.

Substrate	Catalyst	Time	Conversion (%)	Selectivity (%)	
				Epoxide	Others
	PMA/KAP	6	70.2	>99	–
	PMA-(PPh ₃) ₃	3	60.2	34.0	66.0 ^a
	PMA/KAP	6	88.7	16.4	83.6 ^a
	PMA/KAP	6	10.6	>99	–
	PMA/KAP	6	76.2	>99	–
	PMA/KAP	9	43.0	27.3	72.7 ^b
	PMA/KAP	9	68.1	7.3	92.7 ^b
	PMA/KAP	9	27.1	2.6	97.4 ^c

Reaction conditions: catalyst 10 mg, substrate 1 mmol, H₂O₂ 3 mmol, temperature 70 °C, EAC 2 ml.^a 1,2-Hexanediol.^b Benzaldehyde.^c cyclohexane-1,2-diol (5.1%)+2-cyclohexen-1-ol (23.9%)+2-cyclohexene-1-one (68.4%).**Fig. 8.** (A) Leaching experiments of catalyst PMA/KAP in H₂O₂/EAC and H₂O₂/AN. Dashed lines indicate the conversions after the removal of the catalysts. (B) Recycling experiments of cyclooctene with catalyst PMA/KAP in H₂O₂/EAC and H₂O₂/AN respectively. Reaction conditions are analogous to those in Table 1.

H₂O₂/EAC system under the given reaction conditions. The slightly decrease in catalytic activity might be caused by the adsorption of trace amount of reactants or products on the surface of PMA/KAP. As for the H₂O₂/AN system, deactivation of PMA/KAP can be observed when the catalyst is reused for the second run. These results suggest that the types of solvent media have significant effect on the stability of PMA/KAP catalyst during the oxidation process of olefins with H₂O₂.

Solid ³¹P MAS-NMR was carried out to characterize the used PMA/KAP catalyst, which was recovered from the H₂O₂/EAC or the H₂O₂/AN system. As shown in Fig. 9, the ³¹P NMR signals belonged to PMA units have disappeared for the catalyst recovered from H₂O₂/AN, while the signals of the catalyst recovered from H₂O₂/EAC are quite consistent with the fresh catalyst, establish-

ing that PMA can be retained well on the KAP support when the solid catalyst is operated in the system of H₂O₂/EAC. It is worth to mention that there is almost no obvious change for the ³¹P NMR signals belonged to phosphine ligands between the used PMA/KAP catalysts (recovered either from H₂O₂/EAC or from H₂O₂/AN) and the fresh catalyst, revealing that the state of P species for the KAP support is well kept during the catalytic oxidation process.

In order to further understand the effect of solvent/oxidant on the catalytic properties of PMA/KAP catalyst, liquid ³¹P NMR was used to characterize the homogeneous PPh₃, PMA and PMA-(PPh₃)₃ in CD₃CN (or in CD₃CN/H₂O₂). As shown in Fig. 10, the P signal of PPh₃ ligand (dissolved in CD₃CN) appears at -5.58 ppm, and it shifts to 35.81 ppm after treating with H₂O₂ due to the formation of OPPh₃. Similarly, the P signal of PMA shifts from -3.53 ppm

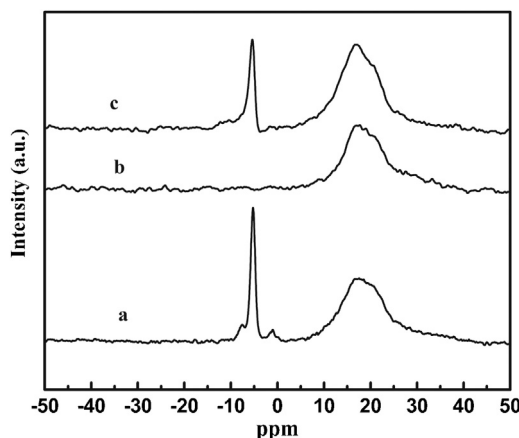


Fig. 9. Solid ³¹P MAS-NMR of (a) fresh PMA/KAP, (b) PMA/KAP recovered from $\text{H}_2\text{O}_2/\text{AN}$ and (c) PMA/KAP recovered from $\text{H}_2\text{O}_2/\text{EAC}$.

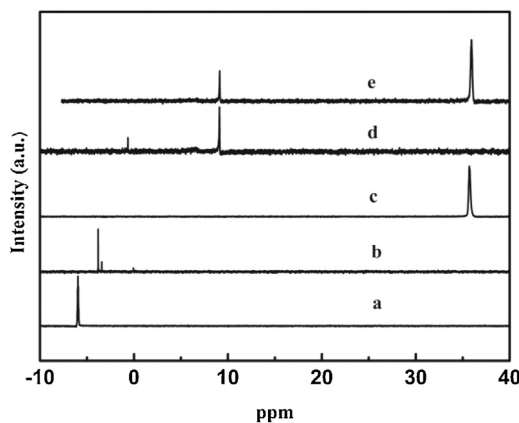


Fig. 10. ³¹P NMR of (a) PPh_3 (b) PMA (c) $\text{PPh}_3 + 0.3 \text{ ml } \text{H}_2\text{O}_2$ aqueous (d) $\text{PMA} + 0.3 \text{ ml } \text{H}_2\text{O}_2$ aqueous (e) $\text{PMA-(PPh}_3)_3 + 0.3 \text{ ml } \text{H}_2\text{O}_2$ aqueous in CD_3CN .

to 9.21 ppm after treating with H_2O_2 , which can be attributed to the formation of degraded product of $(\text{PO}_4[\text{MoO(O}_2)_2]_4)^{3-}$ [36]. For complex $\text{PMA-(PPh}_3)_3$, the P signals for PMA and PPh_3 ligand shift to 9.21 ppm (from -5.53) and to 35.81 ppm (from -5.58), respectively, after treating them with excess H_2O_2 . That is to say, in the system of $\text{H}_2\text{O}_2/\text{AN}$, $\text{PMA-(PPh}_3)_3$ can be rapidly dissolved/degraded into smaller species of $(\text{PO}_4[\text{MoO(O}_2)_2]_4)^{3-}$ and OPPh_3 species. On the basis of these results, it can be deduced that the deactivation of PMA/KAP catalyst in the system of $\text{H}_2\text{O}_2/\text{AN}$ should be also caused by the formation of degraded $(\text{PO}_4[\text{MoO(O}_2)_2]_4)^{3-}$ species, which are easily leached from the solid KAP support.

It should be pointed out here that $\text{PMA-(PPh}_3)_3$ complexes are nearly insoluble when EAC is used as solvent medium, although PPh_3 ligands are easily dissolved in EAC. Upon adding a certain amount of H_2O_2 aqueous solution, $\text{PMA-(PPh}_3)_3$ complexes dissolve partially. After standing for a while, two separating phase, organic phase (EAC layer) and aqueous phase ($\text{H}_2\text{O}_2/\text{H}_2\text{O}$ layer) can be observed. On the basis of the FT-IR results (Fig. 11) and the related literatures [37], it can be concluded that PMA units and $(\text{PO}_4[\text{MoO(O}_2)_2]_4)^{3-}$ species are present in the EAC layer and the $\text{H}_2\text{O}_2/\text{H}_2\text{O}$ layer, respectively. These results suggest that using EAC as solvent medium (rather than AN) can decrease the converting rate of $\text{PMA-(PPh}_3)_3$ complexes to $(\text{PO}_4[\text{MoO(O}_2)_2]_4)^{3-}$ species. This might be mainly due to the fact that EAC has weaker polarity and lower ability of solvent-coordination in comparison with AN. Similar phenomena have already been reported in literature [31], and it was proposed that $[\text{Tp}^{\text{iPr}}\text{MoO}(\text{OPR}_3)\text{X}]$ compound ($\text{Tp}^{\text{iPr}}=\text{hydrotris(3-isopropylpyrazol-1-yl)} \text{ borate; X=Cl}^-$, pheno-

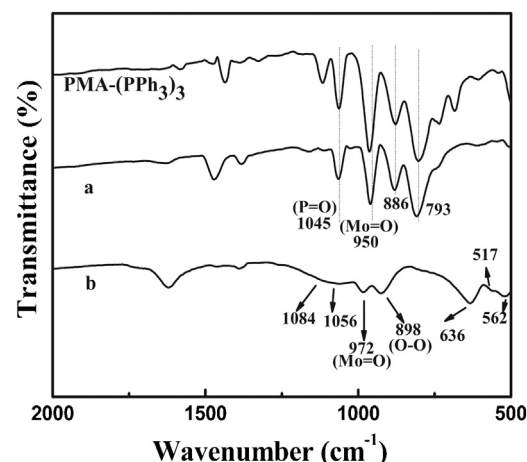


Fig. 11. The FT-IR spectra of $\text{PMA-(PPh}_3)_3$, dissolved in $\text{H}_2\text{O}_2/\text{EAC}$. (a) Precipitation obtained by adding Bu_4NBr in EAC layer, and (b) solid obtained by drying the $\text{H}_2\text{O}_2/\text{H}_2\text{O}$ layer.

lates, thiolates) dissolves easily in the presence of coordinating solvents like AN and DMF, which can form $[\text{Tp}^{\text{iPr}}\text{MoO}(\text{solv})]$ and OPR_3 species rapidly. In the case of noncoordinating solvents, such as CHCl_3 , EAC et al., the structure of the compound can be kept well.

Concerning the relatively high stability/recyclability of PMA/KAP in the system of $\text{H}_2\text{O}_2/\text{EAC}$, it can be imagined that the degradation of PMA to $(\text{PO}_4[\text{MoO(O}_2)_2]_4)^{3-}$ has been completely inhibited when PMA units are introduced into the surface/pores of KAP support, as already confirmed by the above solid ³¹P NMR results. Obviously, the physical/chemical environment of PMA units are different between PMA/KAP and $\text{PMA-(PPh}_3)_3$ complex. During the catalytic oxidation progress, the PPh_3 ligands in $\text{PMA-(PPh}_3)_3$ could be easily converted to OPPh_3 , while the decomposition of $\text{PMA-(PPh}_3)_3$ complexes occurred rapidly. These results suggest that the interaction between the OPPh_3 ligands and PMA units should be not very strong, which could not inhibit the decomposition of PMA during the catalytic reaction course. For PMA/KAP catalyst, it was known that the P-containing ligands are also present in the form of OPPh_3 as revealed by the XPS and NMR results. The main feature KAP support is that the OPPh_3 ligands have been linked through $\text{Ph}-(\text{CH}_2)_x-$ bridges, resulting in the formation of three-dimensional network. In this case, the porous framework of KAP support, which contains numerous bridge-linked phosphine ligands, can be regarded as multi-dentate phosphine ligands with delocalized electrons, just like a steric pocket with low-electron density [31,35]. Associated with the relatively high stability of PMA/KAP catalyst, it can be deduced that the introduced PMA unit might be stabilized by such steric pocket by building multiple weak coordination interactions between the PMA unit and the framework of KAP containing numerous OPPh_3 ligands.

4. Conclusions

PMA functionalized KAP catalyst was synthesized successfully and applied into the oxidation/epoxidation of olefins with H_2O_2 as oxidant. It is found that the resultant PMA/KAP catalyst can perform relatively high activity and stability for the epoxidation of olefins when using EAC as the reaction media. The relative good stability of PMA/KAP catalyst can be mainly assigned to the presence of multiple bridge-linked phosphine ligands dispersed in the bulky KAP support, which can produce a steric pocket with low-electron density for stabilizing the introduced PMA units through multiple weak interaction between the PMA unit and the KAP support.

Acknowledgment

Financial support from the National Natural Science Foundation of China (No. 21173100 and 21320102001) is gratefully acknowledged.

References

- [1] B. Li, F. Su, H. Luo, L. Liang, B. Tan, *Micropor. Mesopor. Mat.* 138 (2011) 207–214.
- [2] X. Du, Y. Sun, B. Tan, Q. Teng, X. Yao, C. Su, W. Wang, *Chem. Commun.* 46 (2010) 970–972.
- [3] D. Dang, P. Wu, C. He, Z. Xie, C. Duan, *J. Am. Chem. Soc.* 132 (2010) 14321–14323.
- [4] B. James, R. Holst, A.I. Cooper, *Adv. Mater.* 22 (2010) 5212–5216.
- [5] H. Furukawa, O.M. Yaghi, *J. Am. Chem. Soc.* 131 (2009) 8875–8883.
- [6] R.W. Tilford, W.R. Gemmill, H.z. Lye, J.J. Lavigne, *Chem. Mater.* 18 (2006) 5296–5301.
- [7] C. Zhao, L. Zhong, *J. Phys. Chem. C* 113 (2009) 16860–16862.
- [8] J. Jiang, F. Su, A. Trewin, C.D. Wood, H. Niu, Y.Z. Khimayk, J.T.A. Jones, A.I. Cooper, *J. Am. Chem. Soc.* 130 (2008) 7710–7720.
- [9] J. Weber, N. Du, M.D. Guiver, *Macromolecules* 44 (2011) 1763–1767.
- [10] J. Lee, C.D. Wood, D. Bradshaw, M.J. Rosseinsky, A.I. Cooper, *Chem. Commun.* (2006) 2670–2672.
- [11] L. Chen, Y. Honsho, S. Seki, D. Jiang, *J. Am. Chem. Soc.* 132 (2010) 6742–6748.
- [12] J. Jiang, C. Wang, A. Laybourn, T. Hasell, R. Clowes, Y.Z. Khimayk, J. Xiao, S.J. Higgins, D.J. Adams, A.I. Cooper, *Angew. Chem. Int. Ed.* 50 (2011) 1072–1075.
- [13] L. Chen, Y. Yang, D. Jiang, *J. Am. Chem. Soc.* 132 (2010) 9138–9143.
- [14] H.J. Mackintosh, P.M. Budd, N.B. McKeown, *J. Mater. Chem.* 18 (2008) 573–578.
- [15] A.M. Shultz, O.K. Farha, J.T. Hupp, S.T. Nguyen, *Chem. Sci.* 2 (2011) 686.
- [16] Z. Xie, C. Wang, K.E. deKrafft, W. Lin, *J. Am. Chem. Soc.* 133 (2011) 2056–2059.
- [17] B. Li, R. Gong, W. Wang, X. Huang, W. Zhang, H. Li, C. Hu, B. Tan, *Macromolecules* 44 (2011) 2410–2414.
- [18] B. Li, Z. Guan, W. Wang, X. Yang, J. Hu, B. Tan, T. Li, *Adv. Mater.* 24 (2012) 3390–3395.
- [19] R. Dawson, L.A. Stevens, T.C. Drage, C.E. Snape, M.W. Smith, D.J. Adams, A.I. Cooper, *J. Am. Chem. Soc.* 134 (2012) 10741–10744.
- [20] M. Jiang, Y. Ding, L. Yan, X. Song, R. Lin, *Chin. J. Catal.* 35 (2014) 1456–1464.
- [21] N. Maksimchuk, M. Timofeeva, M. Melgunov, A. Shmakov, Y. Chesarov, D. Dybtsev, V. Fedin, O. Kholdeeva, *J. Catal.* 257 (2008) 315–323.
- [22] A. Bordoloi, F. Lefebvre, S. Halligudi, *J. Catal.* 247 (2007) 166–175.
- [23] J. Kasai, Y. Nakagawa, S. Uchida, K. Yamaguchi, N. Mizuno, *Chem. Eur. J.* 12 (2006) 4176–4184.
- [24] W. Gao, X. Sun, H. Niu, X. Song, K. Li, H. Gao, W. Zhang, J. Yu, M. Jia, *Micropor. Mesopor. Mat.* 213 (2015) 59–67.
- [25] K. Yamaguchi, C. Yoshida, N. Mizuno, *J. Am. Chem. Soc.* 127 (2005) 530–531.
- [26] Dean C. Duncan, C.R. Chambers, Eric Hecht, Craig L. Hill, *J. Am. Chem. Soc.* 117 (1995) 681–691.
- [27] N. Melanie Gresley, W.P. Griffith, A.C. Laemmel, H.I.S. Nogueira, B.C. Parkin, *J. Mol. Catal. A: Chem.* 117 (1997) 185–198.
- [28] W. He, F. Zhang, H. Li, *Chem. Sci.* 2 (2011) 961–966.
- [29] D.G. Larrude, M.E.H. Maia Costa, F.H. Monterio, F.L. Freire Jr., *J. Appl. Phys.* 111 (2012) 064315.
- [30] M. Nakayama, T. Ii, K. Ogura, *J. Mater. Res.* 18 (2003) 2509–2514.
- [31] A.J. Millar, C.J. Doonan, P.D. Smith, V.N. Nemykin, P. Basu, C.G. Young, *Chem. Eur. J.* 11 (2005) 3255–3267.
- [32] J. Leppin, C. Forster, K. Heinze, *Inorg. Chem.* 53 (2014) 12416–12427.
- [33] P.D. Smith, A.J. Millar, Ch.G. Young, A. Ghosh, Partha Basu, *J. Am. Chem. Soc.* 122 (2000) 9298–9299.
- [34] C.G. Laughlin, L.J. Young, *Inorg. Chem.* 35 (1996) 1050–1058.
- [35] V.N. Nemykin, J. Laskin, P. Basu, *J. Am. Chem. Soc.* 126 (2004) 8604–8605.
- [36] Ji. Hu, R.C. Burns, *J. Mol. Catal. A: Chem.* 184 (2002) 451–464.
- [37] Y. Ding, B. Ma, Q. Gao, G. Li, L. Yan, J. Suo, *J. Mol. Catal. A: Chem.* 230 (2005) 121–128.